DOI: http://dx.doi.org/10.7551/978-0-262-31050-5-ch043

Evolutionary Design and Experimental Validation of a Flexible Caudal Fin for Robotic Fish

Anthony J. Clark, Jared M. Moore, Jianxun Wang, Xiaobo Tan and Philip K. McKinley

BEACON Center for the Study of Evolution in Action
Michigan State University
East Lansing, Michigan, USA 48823
ajc@msu.edu

Abstract

Designing a robotic fish is a challenging endeavor due to the non-linear dynamics of underwater environments. In this paper, we present an evolutionary computation approach for designing the caudal fin of a carangiform robotic fish. Evolutionary experiments are performed in a simulated environment utilizing a mathematical model to approximate the hydrodynamic motion of a flexible caudal fin. With this model, time-consuming computational fluid dynamic simulations can be avoided while maintaining a physically realistic simulation. Two approaches are employed to maximize a robotic fish's average velocity. First, a hill-climbing algorithm is applied to find the optimal stiffness for a fixed shape caudal fin. Next, both fin stiffness and shape are simultaneously optimized with a genetic algorithm. Additionally, simulated caudal fins are compared to physically validated fins, which were fabricated with the aid of a 3D printer and tested on a robotic fish prototype. Results show a correlation between evolved results, model predicted behavior, and physical robot performance with some disparity due to the difficulty in accurately approximating real world performance in a simulation environment. Despite the disparity, evolutionary design is shown to be a viable process.

Introduction

Inspired by natural systems, roboticists have modeled robotic fish with the expectation that they will be as efficient and capable as biological fish. Yet, as is the case with many biomimetic systems, robots are not as proficient as their biological counterparts; the materials and electromechanics that make up a robotic fish simply are not as effective as organic tissue. However, robotic fish do have several advantages over other underwater vehicles types such as propeller-driven robots. First, fewer moving components are necessary, which provides additional space for sensors and reduces power requirements. Additionally, a true-to-life appearance may be less intrusive to the inhabitants of a natural ecosystem. Given these characteristics, robotic fish find applications in scenarios ranging from ecological monitoring to biological studies.

The primary obstacle to developing robotic fish can be attributed to domain uncertainty. Aquatic environments are highly non-linear, which makes the design process a challenging endeavor. For this reason, mathematical models of the hydrodynamic interactions encountered in such environments can improve the design process by providing a means to test design theories. Even with a perfect mathematical model, however, the design process remains a challenge due to the large number of parameters involved in producing realistic motion. Every combination of different materials and electromechanical constraints will produce different performance and requires detailed knowledge of material properties. For example, to fabricate a flexible caudal fin it is necessary to know the modulus of elasticity of the target material. In view of this complexity, it is desirable to create an automated design process that can handle the high-dimensionality of the problem.

Evolutionary computation techniques (genetic algorithms, neuroevolution, genetic programming, and so on) are well suited to such high-dimensional problems. By broadly sampling the solution space, evolutionary algorithms are able to test for and blend the beneficial aspects of unique solutions in order to create efficient mixtures. By integrating a mathematical model into the evaluation phase of an evolutionary algorithm, the idiosyncrasies of an aquatic environment can be exploited to produce effective, even novel, solutions. From such solutions, roboticists can then gain insight into what constitutes a *good* robotic fish design.

In this paper, we propose an evolution-based methodology for the design of a robotic fish caudal fin. Evolutionary optimization occurs in a rigid-body dynamics engine that incorporates a mathematical model of the hydrodynamics associated with a caudal fin. Simulated solutions are first compared to mathematical predictions; a hill-climber algorithm optimizes the stiffness of a fixed shape fin, and the fitness landscape is compared to one derived directly from the model. Next, results are validated by physically realizing a set of fins and testing them on a robotic fish prototype. Fins are fabricated and tested with the aid of a 3D printer and an aquatic test environment. Finally, an evolutionary algorithm is used to optimize the physical characteristics of the caudal fin. Specifically, the stiffness and dimensions of a rectangular caudal fin are simultaneously evolved for a given control pattern. The chief contribution of this work is an evolutionary design method based on recently developed dynamic models that can be adapted into a general robotics engineering process.

Background and Related Work

Robotic fish have practical applications in the study of natural fish morphology and behavior as well as in ecological monitoring. They can provide researchers with controllable imitations to assess the behavior of real fish (Faria et al., 2010), or they can be used in the study of natural evolution and other biological hypotheses (Long et al., 2006, 2011). Recent work, in which robotic fish interact with golden shiners, has shown that a tethered robot with a movable caudal fin can elicit schooling behavior from a natural fish in a water-flow tank (Marras and Porfiri, 2012). When the tail structure remained stationary, however, the live fish did not respond with a schooling behavior, supporting the hypothesis that a biomimetic robot can aid in fish behavioral research. As demonstrated by that work, fish can interact with a realistic robot as if it were a natural fish. With increasingly sophisticated designs, new insight into fish behavior can be gained that would be impossible by simply observing biological fish in the wild or a static lab environment. Aside from biological studies, robotic fish have been proposed as a platform to monitor environmental conditions (Tan et al., 2006), including activities such as oil spill monitoring in the Gulf of Mexico and surveying oxygen content of inland lakes. As robots more closely resemble natural fish, it may be possible to deploy them as mobile sensor platforms that do not disturb local ecosystems.

Research into fin design and fabrication has focused primarily on modeling fin structures found in nature. Each type of swimming locomotion (for example, anguilliform and carangiform) requires a mathematical model to accurately describe the governing dynamics. A ribbon-like fin on a robot with a series of actuators connected by a malleable material has been shown to be capable of replicating the thrust of real fins (Epstein et al., 2006). Further research (Hu et al., 2009; Mason and Burdick, 2000; Chen et al., 2010; Tan et al., 2010) has yielded insight into carangiform fish locomotion, in which forward propulsion is predominantly generated by the caudal fin. Recently, a mathematical model has been proposed to encompass the different aspects of locomotion that apply to a flexible carangiform caudal fin (Wang et al., 2011, 2012).

Morphological evolution has been the focus of an abundance of studies beginning with Sims's evolution of virtual creatures (Sims, 1994). A major hurdle to any simulation-developed solution is how well it transfers into a physical robot. A so-called "reality-gap" arises when solutions that appear to work well in a simulated environment face issues in a physical environment that were either unforeseen or incorrectly modeled (Brooks, 1992; Jakobi, 1998; Koos et al., 2010). Approaches to address this problem include evolving the simulator in conjunction with a robot (Bongard and Lipson, 2004) and directly rewarding solutions for performing similarly in reality and simulation (Koos et al., 2010). In the latter approach, only solutions that have a high transferability (a low disparity between simulation and reality) are deemed highly fit. Further narrowing of the gap is possible by developing accurate models for environmental conditions. In (Gomez and Miikkulainen, 2003), for instance, the authors demonstrated that a detailed simulator can be combined with an evolutionary algorithm to produce controllers for finless rockets, which operate in highly non-linear environments. Recently, the reality gap has expanded to include material properties and their response to specific environmental conditions. Since modeling such interactions at the molecular level is presently intractable, our approach is to integrate evolutionary computation with rigorous mathematical modeling of material properties. Whereas evolutionary computation guides the overall process, engineering is needed to model how constituent materials behave when forces are applied to them, enabling accurate evaluation of the robot in simulation.

Methodology

To create such an environment, we built our simulator on top of a mathematical model and an open source rigid-body dynamics engine, the Open Dynamics Engine (ODE) (Smith, 2012). Additionally, to ensure that results are meaningful, we validated our simulator against fins that were physically tested on a robotic fish prototype.

Mathematical Model

Using rigid-body dynamics, natural caudal fin motion can be approximated by dividing the fin into multiple discrete segments connected by a spring and damping system (Wang et al., 2012). Still, the fluidic motion of a fin during locomotion can be hard to model in simulation and equally as hard to replicate on a physical robot. However, with the advent of 3D printers, we can rapidly test a variety of different materials and discover which are most capable of approximating that motion. Lighthill's Elongated Body Theory of Locomotion (Lighthill, 1971) was proposed to describe the movement patterns of a real fish as if the entire body were flexible. In Lighthill's approach, the movement at any point on a body can be approximated using equations that result in the thrust and movement of that point.

All of the fins in this study were rectangular; we are considering other shapes in our on going investigations. The mathematical model we use to compute the forces produced by rectangular fins is based on Lighthill's theory. In this model, a caudal fin is divided into equal-sized segments and the hydrodynamic forces are evaluated independently for each segment along with an additional force acting at the tip (Wang et al., 2012). The fin segments in the mathematical model are assumed to be connected through a series of spring and dampers that result in a flexible fin structure, as shown in Figure 1.

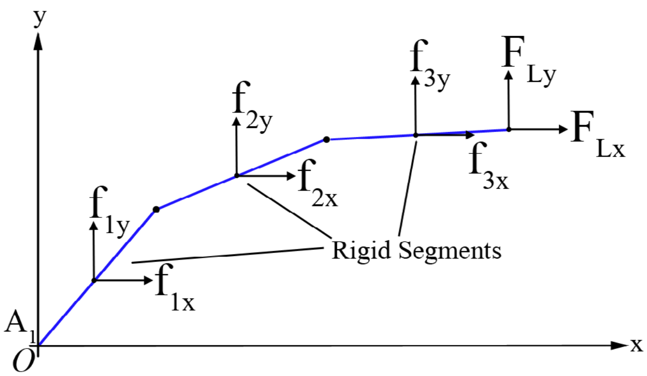

Figure 1: Visual representation of the mathematical model describing the forces acting on the segments of a passive flexible caudal fin.

In the figure, three segments are shown along with the forces that apply to each individual segment. According to the mathematical model, each fin segment generates two component forces, a resistive component and a propulsive component. Each segment experiences hydrodynamic forces described by Equation 1:

$$\vec{f}(\tau) = \begin{pmatrix} f_X(\tau), \\ f_Y(\tau) \end{pmatrix} = -m\frac{d}{dt}(v_\perp \hat{n}), \qquad (1)$$

where m denotes the mass per unit length, τ is the location on the fin where the force acts, and $\hat{n}$ and $v_\perp$, respectively, are the unit direction and velocity perpendicular to the fin. The tip of the final segment experiences an additional force described by Equation 2:

$$\vec{F}_L = \begin{pmatrix} F_{LX} \\ F_{LY} \end{pmatrix} = \left[-\frac{1}{2}mv_\perp^2\hat{m} + mv_\perp v_\parallel \hat{n} \right]_{\tau=L}, \qquad (2)$$

where τ=L represents the posterior end of the fin, and $\hat{m}$ and $v_\parallel$, respectively, are the unit direction and velocity parallel to the fin. These hydrodynamic forces can be calculated given the X and Y of each fin segment over time.

At the base of the fin, which is attached to the body, a motor drives the rhythmic motion in a sinusoidal pattern. The parameters for this sinusoidal motion includes the amplitude, frequency, and bias. Along with a material's dimensions, the Young's modulus of elasticity determines flexibility, which is captured in the parameters for the springs and dampers. This relationship provides a means of transferring simulated designs into real materials using known and inferred properties of materials.

Simulation Environment

In view of the unique challenges associated with modeling the fluid dynamics of an aquatic environment, ODE was used in conjunction with the above mathematical model to approximate the hydrodynamic forces acting on a caudal fin. This method avoids costly computational fluid dynamics calculations. The reduction in computation time is particularly advantageous for evolutionary experiments in which thousands of solutions must be simulated. Consistent with surface-swimming robots, the mathematical model constrains motion to a two-dimensional plane and assumes neutral buoyancy.

The simulated robotic fish is modeled after a physical robotic fish prototype, which was originally constructed to test the performance of different fin dimensions and material stiffnesses. A representation of the virtual model can be seen in Figure 2, showing the main body and a three-segment caudal fin. Fin flexibility was approximated with passive hinges between fin segments governed by predefined spring and damper constraints. This spring system allows the fin to flex at different rates depending on spring and damping coefficients. Rotational movement of the fin is achieved through an actuated hinge connecting the body and first fin segment. The body-fin joint oscillates at 0.9Hz in a 30 degree symmetrical range of motion.

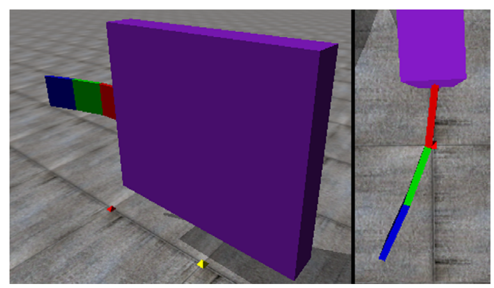

Figure 2: Depiction of the virtual fish model with a three-segment rigid-body caudal fin.

Physical Validation

To validate the proposed method, test fins were fabricated using an Objet Connex350 multi-material 3D printer. Fins were printed with a combination of different physical materials to yield flexibilities that resemble the motion observed in simulation. As demonstrated in (Richter and Lipson, 2011), a 3D printer can considerably improve the efficiency of an experimental design process. Several iterations of printed parts can be fabricated in a matter of hours. The printed fins were attached to a robotic fish prototype and evaluated in an aquatic test environment. An image of the physical robot with attached fin is shown in Figure 3.

Time trials were used to determine the average velocity achieved by each fin, while visual observations helped determine the flexibility of fins during movement. In these physical trials, the height, length, and thickness of each fin were fixed at 2.5, 8.0, and 0.1 cm, respectively. The Young's modulus of elasticity was provided by the manufacturer data sheets. For each of the printed fins, the robot was placed in

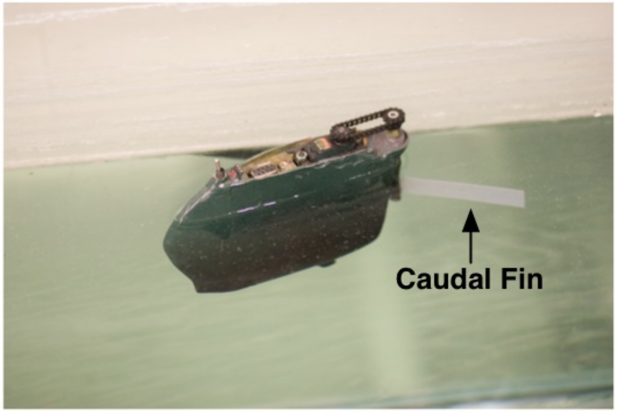

Figure 3: The robotic fish prototype. Movement of the 3D-printed rectangular caudal fin is accomplished using a servo motor with a set range of motion and period of oscillation.

a test tank and allowed to reach a stable swimming speed before the average velocity was computed. The stiffness of each fin can be calculated with Equation 3:

$$K_s = \frac{Edh^3}{12l}, \tag{3}$$

where K_s represents a material's torsion spring constant, d and l denote the height and length of the fin, respectively, E represents Young's modulus of elasticity for the material itself, and h is the thickness of a fin. These values can be directly used in simulation during optimization trials and provide a means of effectively comparing simulation and physical results.

Experiments and Results

The methodology proposed in this paper can be divided into three separate parts: mathematical model validation, physical validation, and evolutionary optimization. We first compared our simulation results with data derived directly from the mathematical model. Next, we performed a similar comparison between simulation and data gathered from physical experiments. Once our simulation environment was validated, we applied evolutionary computation techniques to a flexible fin design process.

Mathematical Model and Simulation

Prior to physical validation and evolutionary experiments, it was important to ensure that our simulation environment matched the mathematical model. Any disparity between simulation and model could signify an error that would make evolutionary results meaningless. With this in mind, two algorithms were employed to optimize the stiffness of the simulated caudal fin. In both experiments, only the Young's modulus was allowed to change.

The first algorithm was a basic hill-climber. For this experiment, 100 independent runs were conducted. Every run was initialized with a different seed and a Young's modulus value chosen uniformly at random from the range [0, 5 GPa]. Every Young's modulus value was evaluated by translating it, with Equation 3, to the spring coefficients that govern caudal fin flexibility. Once the simulated robotic fish was configured, it was allowed to swim for 10 seconds. The fitness of each Young's modulus was computed as the average velocity achieved over this evaluation period. Each hill-climber run began with the evaluation of the randomly-chosen initial Young's modulus value. Subsequent values were generated by displacing the current value by a random number chosen uniformly from a Gaussian distribution with a mean of 0 and a variance of 0.1. The resulting Young's modulus was then evaluated, and the better performing (higher average velocity) value was kept and used to generate the next test case. In each run, this process was repeated until 100 candidate values had been evaluated. Every hill-climber instance converged to an optimum Young's modulus of roughly 1.9 GPa, and given enough time it is suspected that all final values would converge to a single optimal value.

The second algorithm deployed was a conventional genetic algorithm. The primary use of this experiment was to confirm that the simulation environment could be used effectively with an evolutionary algorithm. This experiment comprised 30 independent runs. Each run was seeded with a different value and a population of 125 randomly generated individuals. Every individual was evaluated in a process identical to that used in the hill-climber experiment. The populations were evolved for 100 generations with mutation as the only evolutionary operator. After population initialization, subsequent generations were created by using a three-individual tournament selection process and a Gaussian mutation operator (identical to the hill-climber displacement operator). Additionally, to ensure that the highest fitness individuals were not lost, the most fit 10% of the population was considered elite and copied to the next generation without modification.

Results from the evolutionary experiment closely resembled those of the hill-climber, with the most fit individuals, in every run, having a Young's modulus near 1.9 GPa. Data generated from the mathematical model can be seen in Figure 4, and results from the two simulation experiments are shown Figure 5. The experimental results show that both the hill climber and evolutionary approaches yield near identical solutions (i.e. a Young's modulus of 1.9 GPa). This is an expected result, as both experiments rely on the same simulation environment.

Comparing Figures 4 and 5, a disparity between model and simulation results is apparent. Specifically, the model predicts a maximum velocity of roughly 5.1 cm/s at a Young's modulus near 0.9 GPa, while simulation results achieve a maximum average velocity closer to 1.4 cm/s at a Young's modulus near 1.9 GPa. Despite the differences,

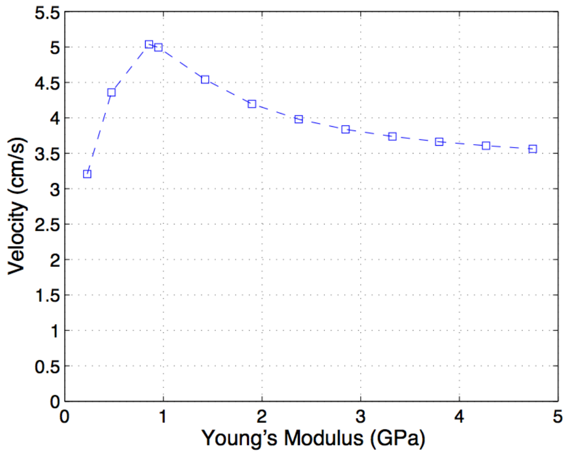

Figure 4: Predicted velocities for different Young's Modulus values from the mathematical model calculations. Note that this assumes that the body is anchored.

both figures show the same trend, in which intermediate values of the Young's modulus produce the fastest robotic fish. Additionally, the disparity between figures can be explained by closer examination of the model and simulator. The most marked differences are that the mathematical model assumes the robotic fish body does not affect caudal fin motion, and the caudal fin segments are without mass. Neither of these assumptions is carried over into the simulation environment, and both of these factors would cause simulated robotic fish to appear *slower* than model data would predict. In the next section, physical results will be examined to determine whether the simulation results are physically meaningful.

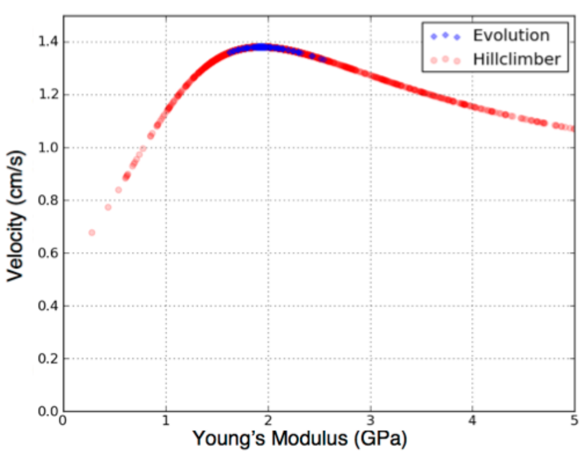

Figure 5: Results of the hill climber and evolutionary runs for determining the optimum stiffness of a fixed dimension fin. Both methods converged on a common stiffness yielding the highest average velocity. Darker shades indicate clustered results from different trials.

Physical Validation

To validate observations taken from simulation, we fabricated caudal fins with a 3D printer and tested them on a robotic fish prototype in an aquatic environment. Six unique fins were printed, each with a different Young's modulus. The materials ranged from extremely flexible (TangoBlackPlus) to nearly inflexible (VeroWhite). Each printed fin was attached to the robot and tested in the aquatic environment; the average velocity was measured over 5 separate trials. The results of this experiment are plotted in Figure 6. Consistent with the predicted performance, the plot shows that an intermediate flexibility produces the highest average velocity. However, direct comparisons between simulation and reality are not possible due to current limitations of the 3D printed materials. Specifically, the materials do not have an exact Young's modulus value, but rather the manufacturer provides a range of possible values for each material (materials properties are not guaranteed to remain constant between print jobs). For example, VeroWhite has a modulus in the range of 2-3 GPa, while the other materials have lower-value ranges.

In view of the fact that the mathematical model, simulation, and physical data are all for fins of identical shape, some comparisons can yet be made. First, the velocity values of the physical robotic fish are closer to mathematical model predictions than they are to simulation results. The data collected from these experiments will be vital in improving the model and simulation environment. In addition, the optimal Young's modulus for all results is in the range of 1-2 GPa. The reason for the disparity in the model predictions was discussed in the previous section, however it is also apparent that simulation results do not perfectly match reality. The maximum velocity of 3.7 cm/s in the physical experiments is nearly twice the maximum simulation velocity. As with the model, certain approximations were made in the simulation environment. For instance, distributed forces were treated as single point forces, and the flexible fin was split into just three segments. By decreasing the size of each segment and increasing the number of segments, the motion and discretization of forces will be more realistic and likely increase the accuracy of the simulation.

As a secondary measure of performance between the simulation and physical experiments, we observed the flexibility of fins as they oscillated. Figure 7 presents a side by side comparison between a simulated flexible caudal fin and the 3D printed version on the robot. Both series of images display the flexibility of a fin as it oscillates. This visual observation helps to reinforce the viability of simulating flexible caudal fins.

Evolution of Fin Morphology

Upon completion of comparisons between mathematical model and simulation results, optimization was expanded into a full evolutionary computation run in which the

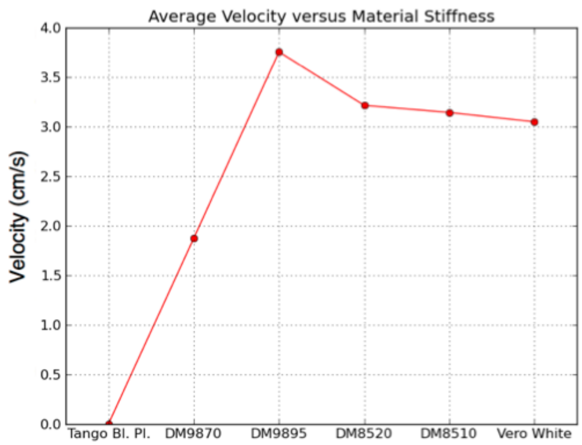

Figure 6: Observed average velocity for different materials used in printed fins. Stiffness increases from left to right in the plot.

Young's modulus and dimensions of a rectangular caudal fin were simultaneously evolved. Fin shape was allowed to evolve under the constraint that the overall area of the length-height face and the thickness of the fin remain fixed. This created a state in which the height of the fin was dependent upon the length of the fin. As such, the two parameters to evolve were the Young's modulus and length of a fin. Practical considerations on the overall dimensions of the fin were also taken into account as a maximum length of 14 cm (length of the robotic fish body) and a minimum length of 4 cm (half the length of previous experiments) were imposed upon evolution. Values outside of this range could suffer from transferability issues given electromechanical constraints such as the maximum torque exerted by a servo. Again, an individual run consisted of 125 individuals evolving for 100 generations. Similar to the previous evolutionary experiments, tournament selection, of size 3, and elitism were used to select the parents for the next generation. Unlike earlier experiments, however, single point crossover was added so that individuals could be generated as a combination of two selected parents. In total, 30 replicate runs were conducted to find the relationship between fin stiffness, fin shape, and average velocity.

From the evolutionary runs, a set of optimum values was found for both the Young's modulus and dimensions of the fin. The Young's modulus found in the trial was 7.55 GPa, and the caudal fin length and height were 14 and 1.43 cm respectively. Hence, the fittest solutions reached the maximum fin length allowed at a cost of fin width. This result was expected, as a longer fin will be able to generate larger propulsive forces, while width has a lesser effect on this force. This characteristic can be seen by close examination of Equation 2, where the length of a fin is a linear factor,

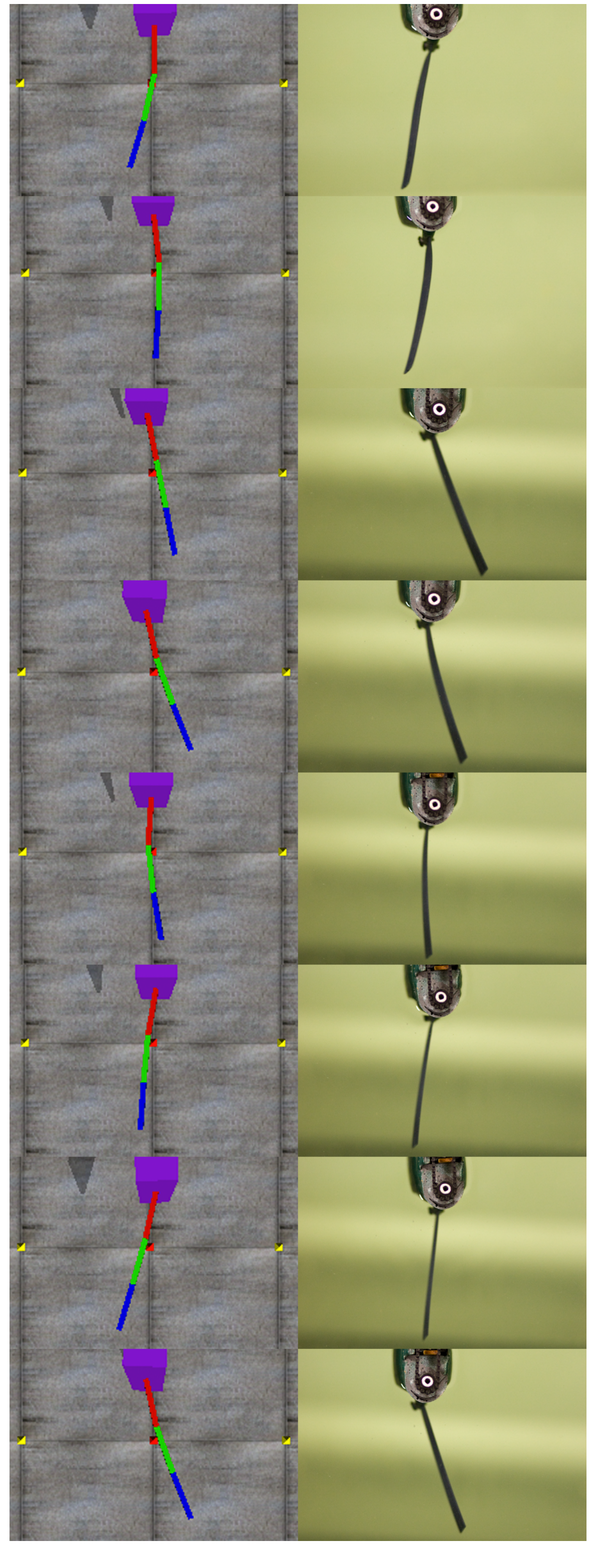

Figure 7: Visual performance of the evolved flexible fin in simulation (left) versus a fabricated flexible fin tested on the prototype robot (right).

and longer fins will have a higher angular velocity near the posterior of the fin.

While the Young's modulus found in the trial is larger than that found in prior experiments, the resulting material stiffness is similar: 1.35×10^{-3} N m for the original experiments, and 1.73×10^{-3} N m for the full evolutionary experiments. This result suggests that a single stiffness value may be adequate for any rectangular caudal fin dimensions. The reason these stiffness values are similar is that as length increased, the Young's modulus also increased to maintain a fairly constant value. Figure 8 presents the three dimensional fitness landscape found in the evolutionary run. As shown, a peak is located at a modulus of elasticity of 7.55 GPa and a length of 14 cm. This combination yielded an average velocity of 2.2 cm/s. This landscape would suggest that for each set of dimensions there is a specific Young's modulus that correlates to the overall best performance for a fin.

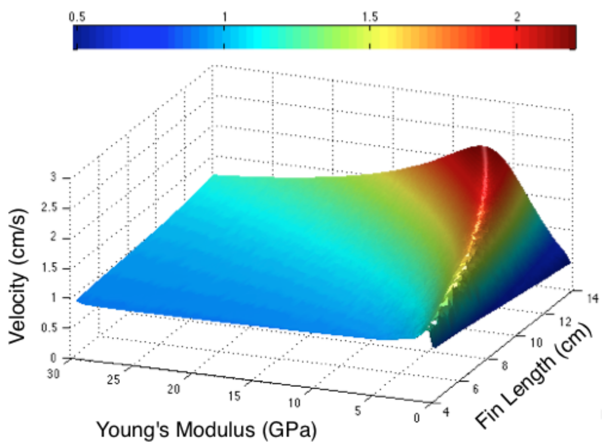

Figure 8: Visualization of the fitness landscape for different shape and stiffness fins. Note that height is dependent upon length in determining shape, therefore, height has been omitted from the data. As the length of the fin increases, the Young's Modulus increases as well to maintain similar stiffness fins for different lengths.

The complex dynamics of an underwater environment make designing efficient robotic fish a challenging engineering endeavor. Considering the difficulty, it is desirable to create an automated design process by which robotic fish can be optimized for a specific task. Making use of the hydrodynamic model for a robotic fish caudal fin, we have shown that an *in silico* process can be used to optimize the Young's modulus of a flexible fin. In simulation, we observed that the optimum Young's modulus is dependent on both the caudal fin motion and dimensions. Specifically, for any combination of fin frequency, amplitude, height, width and length there will be a unique Young's modulus optimum. However, when the Young's modulus was simultaneously evolved with fin shape, we found that the overall resulting fin stiffness exhibited comparable characteristics. Generally, higher values of length and Young's modulus produced faster swimmers.

Conclusion

In this paper, we demonstrated an evolutionary design method for robotic fish caudal fins. We first developed a simulation environment in which unique fin configurations could be tested. The simulation environment was created by combining a rigid-body dynamics engine with a mathematical model of a flexible caudal fin's hydrodynamics. To test the simulation environment, we first implemented a hill-climber algorithm. Given a fixed fin shape and control pattern, the hill-climber algorithm mapped-out the fitness landscape for fin stiffness vs. velocity. These results were compared to data generated directly from the model, which confirmed that the simulation and the mathematical model have comparable dynamics, although the absolute values differ.

Hill-climber results were further validated through comparisons with physical experiments. With the aid of a 3D printer, an aquatic test environment, and a robotic fish prototype, we conducted a series of velocity tests for several 3D-printed fins. All fins were identical in shape, but had stiffness values (i.e. Young's modulus) ranging from very low to nearly inflexible. Plots of stiffness vs. velocity for the mathematical model, simulation, and physical experiments all showed a similar trend in which average velocity was maximal for intermediate caudal fin flexibility. This result demonstrates that it is possible for a simulation environment to capture key aspects of the dynamics of flexible materials.

To simultaneously optimize several fin parameters, we progressed from the hill-climber experiments to an evolutionary algorithm. A conventional genetic algorithm was used to evolve both the Young's modulus and shape of a fin. From this series of experiments, we found that the most fit fins generally evolved to be as long as possible while maintaining a fairly constant stiffness value. This result is consistent with the fact that longer fins generally produce larger propulsive forces. Additionally, our results showed that for each fin shape and control pattern there is an associated optimal Young's modulus.

The simulated and physical results discussed in this paper demonstrate the effectiveness of an evolutionary based approach given the high dimensionality of the solution space. To continue this research, our future work will focus on improving the design process. First, basic assumptions central to the hydrodynamic model will be removed. For instance, the body will no longer be considered anchored and the fins no longer without mass. Our rigid-body simulator will also be improved by converting our single-point forces to more accurate distributed forces. These improvements alone are likely to increase the accuracy of the simulation and in turn facilitate the transfer of simulated solutions to reality. Next, we will gradually relax the constraints placed on evolution. In biological fish, caudal fins predominantly increase in height towards the posterior, and accordingly evolution should be allowed to evolve non-rectangular fins. Additionally, due to fin motion being a key component of optimization, it is likely that evolution will be able to find more appropriate control patterns. Ultimately, the goal is to simultaneously evolve as many aspects of the robotic fish as possible in a process that can be generalized to any non-linear robotic environment.

Acknowledgements

The authors gratefully acknowledge the contributions and feedback on the work provided by Professor Janette Boughman, members of the Software Engineering and Network Systems Laboratory, the Smart Microsystems Laboratory, the Digital Evolution Laboratory, and the BEACON Center at Michigan State University. This work was supported in part by National Science Foundation grants CNS-1059373, CNS-0915855, DBI-0939454, CCF-0820220, IIS-0916720, ECCS-1050236, ECCS-1029683 and CNS-0751155; and by U.S. Army Grant W911NF-08-1-0495.

References

Bongard, J. C. and Lipson, H. (2004). Once more unto the breach: Co-evolving a robot and its simulator. In *Proceedings of the Ninth International Conference on the Simulation and Synthesis of Living Systems*, pages 57–62, Boston, Massachusetts, USA.

Brooks, R. A. (1992). Artificial life and real robots. In *Proceedings of the First European Conference on Artificial Life*, pages 3–10. MIT Press, Cambridge, MA.

Chen, Z., Shatara, S., and Tan, X. (2010). Modeling of biomimetic robotic fish propelled by an ionic polymer metal composite caudal fin. *IEEE/ASME Transactions on Mechatronics*, 15(3):448–459.

Epstein, M., Colgate, J., and MacIver, M. (2006). Generating thrust with a biologically-inspired robotic ribbon fin. In *Proceedings of the 2006 IEEE/RSJ International Conference on Intelligent Robots and Systems*, pages 2412 –2417, Beijing, China.

Faria, J., Dyer, J., Clément, R., Couzin, I., Holt, N., Ward, A., Waters, D., and Krause, J. (2010). A novel method for investigating the collective behaviour of fish: introducing 'Robofish'. *Behavioral Ecology and Sociobiology*, 64:1211–1218.

Gomez, F. J. and Miikkulainen, R. (2003). Active guidance for a finless rocket using neuroevolution. In *Proceedings of the 2003 Genetic and Evolutionary Computation Conference*, pages 2084–2095, San Francisco, California, USA. Morgan Kaufmann.

Hu, Q., Hedgepeth, D., Xu, L., and Tan, X. (2009). A framework for modeling steady turning of robotic fish. In *Proceedings of the 2009 IEEE International Conference on Robotics and Automation*, pages 2669 –2674, Kobe, Japan.

Jakobi, N. (1998). Running across the reality gap: Octopod locomotion evolved in a minimal simulation. In *Proceedings of the First European Workshop on Evolutionary Robotics*, pages 39–58, Paris, France. Springer-Verlag.

Koos, S., Mouret, J. B., and Doncieux, S. (2010). Crossing the reality gap in evolutionary robotics by promoting transferable controllers. In *Proceedings of the 2010 ACM Genetic and Evolutionary Computation Conference*, pages 119–126, Portland, Oregon, USA. ACM.

Lighthill, M. J. (1971). Large-amplitude elongated-body theory of fish locomotion. *In Proceedings of the Royal Society of London. Series B, Biological Sciences*, 179(1055):125–138.

Long, J. H., Koob, T. J., Irving, K., Combie, K., Engel, V., Livingston, N., Lammert, A., and Schumacher, J. (2006). Biomimetic evolutionary analysis: testing the adaptive value of vertebrate tail stiffness in autonomous swimming robots. *Journal of Experimental Biology*, 209(23):4732.

Long, J. H., Krenitsky, N. M., Roberts, S. F., Hirokawa, J., de Leeuw, J., and Porter, M. E. (2011). Testing biomimetic structures in bioinspired robots: How vertebrae control the stiffness of the body and the behavior of fish-like swimmers. *Integrative and Comparative Biology*, 51(1):158–75.

Marras, S. and Porfiri, M. (2012). Fish and robots swimming together: attraction towards the robot demands biomimetic locomotion. *Journal of The Royal Society Interface*.

Mason, R. and Burdick, J. (2000). Experiments in carangiform robotic fish locomotion. In *Proceedings of the 2000 IEEE International Conference on Robotics and Automation*, volume 1, pages 428–435.

Richter, C. and Lipson, H. (2011). Untethered hovering flapping flight of a 3d-printed mechanical insect. *Artif. Life*, 17(2):73–86.

Sims, K. (1994). Evolving virtual creatures. In *Proceedings of the 21st Annual Conference on Computer Graphics and Interactive Techniques*, SIGGRAPH '94, pages 15–22, New York, NY, USA. ACM.

Smith, R. (2012). Open Dynamics Engine, http://www.ode.org/.

Tan, X., Carpenter, M., Thon, J., and Alequin-Ramos, F. (2010). Analytical modeling and experimental studies of robotic fish turning. In *Proceedings of the 2010 IEEE International Conference on Robotics and Automation*, pages 102–108, Anchorage, Alaska, USA.

Tan, X., Kim, D., Usher, N., Laboy, D., Jackson, J., Kapetanovic, A., Rapai, J., Sabadus, B., and Zhou, X. (2006). An autonomous robotic fish for mobile sensing. In *Proceedings of the 2006 IEEE/RSJ International Conference on Intelligent Robots and Systems*, pages 5424–5429, Beijing, China.

Wang, J., Alequin-Ramos, F., and Tan, X. (2011). Dynamic modeling of robotic fish and its experimental validation. In *Proceedings of the 2011 IEEE/RSJ International Conference on Intelligent Robots and Systems*, pages 588–594, San Francisco, California, USA.

Wang, J., McKinley, P. K., and Tan, X. (2012). Dynamic modeling of robotic fish with a flexible caudal fin. In *Proceedings of the 5th Annual Dynamic Systems and Control Conference*, Ft. Lauderdale, Florida, USA. Accepted for publication.